



THE UNIVERSITY *of* EDINBURGH

Edinburgh Research Explorer

Assessing cellular automata based models using partial differential equations

Citation for published version:

Doeschl, A, Davison, M, Rasmussen, H & Reid, G 2004, 'Assessing cellular automata based models using partial differential equations' *Mathematical and computer modelling*, vol 40, no. 9-10, pp. 977-994., 10.1016/j.mcm.2004.04.004

Digital Object Identifier (DOI):

[10.1016/j.mcm.2004.04.004](https://doi.org/10.1016/j.mcm.2004.04.004)

Link:

[Link to publication record in Edinburgh Research Explorer](#)

Document Version:

Publisher final version (usually the publisher pdf)

Published In:

Mathematical and computer modelling

Publisher Rights Statement:

@ 2004 Elsevier Ltd.

General rights

Copyright for the publications made accessible via the Edinburgh Research Explorer is retained by the author(s) and / or other copyright owners and it is a condition of accessing these publications that users recognise and abide by the legal requirements associated with these rights.

Take down policy

The University of Edinburgh has made every reasonable effort to ensure that Edinburgh Research Explorer content complies with UK legislation. If you believe that the public display of this file breaches copyright please contact openaccess@ed.ac.uk providing details, and we will remove access to the work immediately and investigate your claim.





Assessing Cellular Automata Based Models Using Partial Differential Equations

A. DOESCHL*, M. DAVISON, H. RASMUSSEN AND G. REID

Department of Applied Mathematics, University of Western Ontario
London, Ontario, Canada, N6A 5B7

(Received September 2002; revised and accepted April 2004)

Abstract—This paper presents a novel method of assessing cellular automata based models. The cellular model considered in this paper was designed to simulate sediment transport and topographic changes in rivers. It is demonstrated how prior knowledge about partial differential equations and their solution schemes can be used to provide deeper insight into the performance of two numerical implementations for this cellular model. Assessment of the implementations as solution schemes of the derived partial differential equations showed that the cellular model is robust for two numerical implementations, one of which is superior in terms of accuracy, stability and convergence. In comparison with more sophisticated solution methods, both implementations return accurate results. This study encourages the further application of cellular automata based models to complex problems.
© 2004 Elsevier Ltd. All rights reserved.

Keywords—Cellular automata, Numerical models of fluvial processes, Partial differential equations.

1. INTRODUCTION

Mathematical and numerical models have become a common tool for studying complex natural phenomena. Traditional modeling approaches aim to identify the governing mechanical processes and represent them by systems of partial and integro-differential equations. In most cases, these can only be solved by numerical approximations. This reductionist modeling approach has proved greatly successful in simulating the behavior of many complex systems. The formulation and assessment of numerical solution schemes has become a major research field. However, the detailed representation of the governing physical processes associated with the reductionist approach requires expert numerical skills often combined with large amounts of computational resources. Moreover, interpretation of the model results is often obscured by the strong interaction between several complex phenomena, which are simultaneously represented in the model.

In recent decades, cellular automata models have emerged as an alternative modeling approach [1]. Instead of reducing the system to its fundamental components, cellular automata models focus on key aspects of the system and use simple rules to represent them quantitatively.

*Author to whom all correspondence should be addressed. Current address: Animal Nutrition and Health Department, Scottish Agricultural College, Bush Estate, Penicuik, EH26 0PH, UK.

They don't reproduce the detailed behavior of a system, but aim to capture its relevant characteristics and produce the enigmatic behaviors of interest [2]. Cellular automata portray the system by discrete sets of cells which interact with each other according to their properties and according to rules that represent the system's mechanics in a highly simplified manner. This discrete, simplistic representation certainly lacks the microscopic fidelity of reductionist models, but the simplicity of the formal representations of the modeled processes increases the clarity of insight and explanatory power regarding the mechanisms causing a poorly understood phenomenon [2]. In systems with complicated boundary conditions or domain geometry, cellular models can be much faster than reductionist models [3]. These models are easy to construct and modify, and so offer many possibilities for exploring system behavior.

Both modeling approaches have their obvious advantages and have contributed a great deal to a better understanding of many natural and artificial systems. However, both approaches also demand a high price for their advantages. Reductionist models often obscure the fundamental aspects that control the overall behaviour of the modelled system. Further, they reach their limits when the underlying physical principles of the considered phenomenon are unknown or when systems become too complex to solve by analytical or numerical means. Cellular models, which concentrate on key aspects of the modelled system, are generally difficult to validate. The assessment of these models is often restricted to visualization of the results and lacks rigorous analysis. Alternatively, appropriate assessment requires the development of new assessment methods or a deep understanding of already existing methods from other research fields.

To enhance the recognition of the key aspects and to relieve the burden of lengthy computations, many reductionist models depicted by complex systems of partial differential equations have been simplified to cellular automata [4]. The question arises, whether insights obtained from the traditional reductionist modeling approach can also contribute a more rigorous assessment of cellular models. The aim of this paper is to demonstrate how partial differential equations can be used to assess numerical schemes arising from a mathematical cellular automata model.

The present study focuses on a cellular model for sediment transport and topographic changes in river beds. The model was generated to examine the essential criteria for the establishment and propagation of braided channel patterns in rivers [5]. It has been applied to study the impact of environmental change in catchment areas (see [6]) and the role of vegetation for bank stability [7]. Due to the simplified representation of the governing processes, the model has provoked intense debates in the fluvial community [7]. Whereas many are attracted by the simple, fast computations, others are skeptical about the validity of the model results. The model predictions have been assessed according to methods ranging from visualization, dynamical systems theory [8,9] and fractal analysis [10] to statistics [11]. But questions about the accuracy, convergence, and stability of the model predictions or the model's robustness to various implementations cannot be answered by these methods.

For the purpose of this study it is convenient to reduce the original two-dimensional model to one dimension. In one dimension, the model no longer represents braided river processes; instead, it predicts the evolution of a longitudinal river profile through the propagation of water and sediment. Although this is a high price to pay, reduction to one spatial dimension facilitates the model assessment in terms of robustness, accuracy, and stability and provides insight into the model performance that would be more difficult to obtain in higher dimensions. Two rival numerical implementations will be presented, provoking questions about the advantages of either approach and about the model's robustness to different numerical implementations. These questions are tackled by deriving partial differential equations from both implementations and by assessing the numerical models as solution schemes of the corresponding equations. Depending on the parameter choice, the model can be either linear or nonlinear. The investigations start with the linear model, for which a variety of rigorous assessment methods for numerical solution schemes can be applied, and continue with a more realistic nonlinear model for this phenomenon. An outline of this paper is sketched in Figure 1.

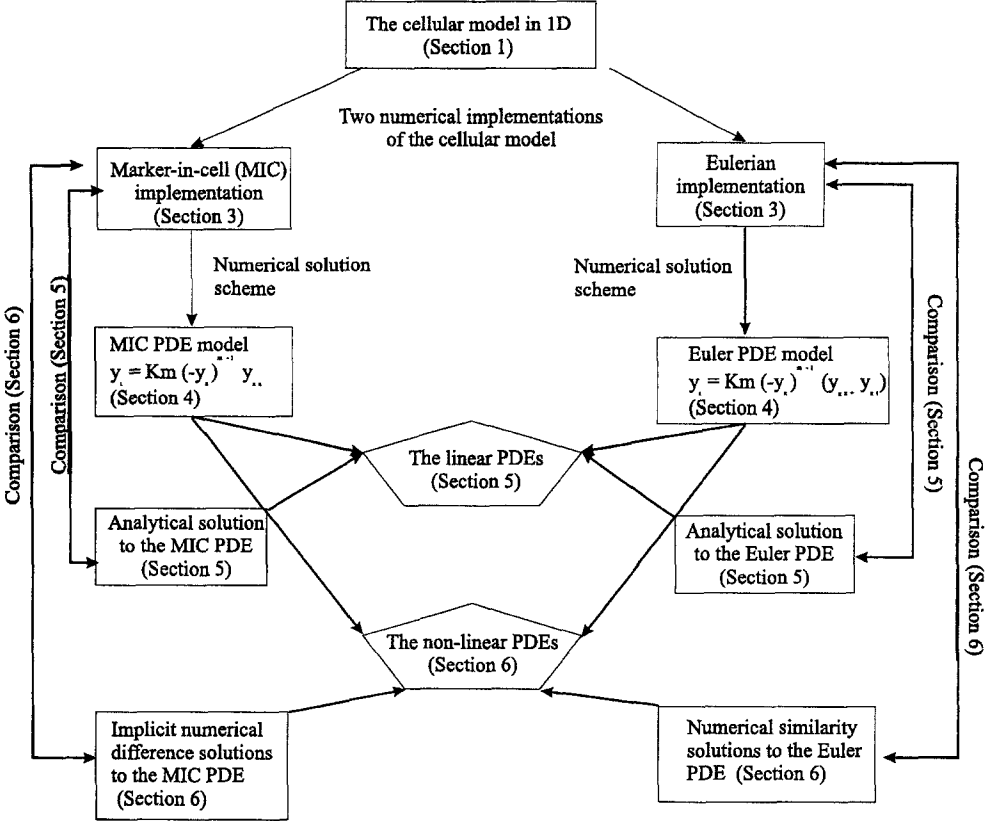


Figure 1. Schematic diagram of the contents of this paper.

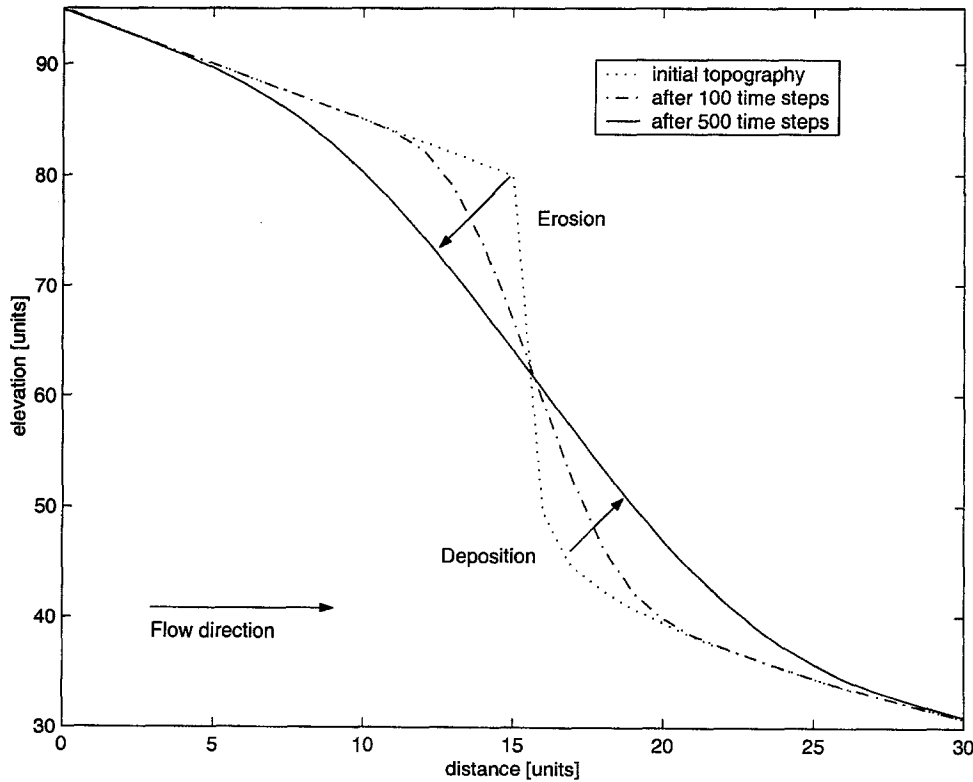


Figure 2. Schematic diagram of the temporal evolution of a river bed profile.

2. THE CELLULAR MODEL IN ONE DIMENSION

In one dimension, the model mimics the following simple process: starting with a longitudinal initial profile of a riverbed, water and sediment introduced at the upstream end propagate in the downstream direction. The propagation of sediment causes erosion and deposition at different locations, which changes the bed profile (see Figure 2). The cellular model divides the bed profile into a sequence of discrete cells of equal length Δx . Each cell of the one-dimensional lattice has coordinates (x, y) , where x is the location of the cell center and y is the average bed elevation in the cell length. The model variables are the water flux Q and the sediment flux M . The propagation of water and sediment is discretized by transferring both quantities from cell to cell. The propagation of water follows the principle of conservation of mass: the amount of water that enters a cell also leaves the cell during the same time step. In one dimension, this implies a constant water flux Q . The sediment transport between adjacent cells obeys the following rule, which was deduced from empirical studies [8,12],

$$M = \begin{cases} K(QS)^m, & \text{if } S \leq 0, \\ 0, & \text{if } S > 0. \end{cases}$$

The parameter K in the above equation is an unconstrained scaling constant and the exponent m is positive. The variable S is the slope between adjacent cells. Empirical studies [12,13] suggest values between $m = 5/3$ and $m = 5/2$. Since, in one dimension, Q is constant, the above equation simplifies to

$$M = \begin{cases} \tilde{K} S^m, & \text{if } S \geq 0, \\ 0, & \text{if } S < 0. \end{cases} \quad (1)$$

The cell elevation change during a time step is denoted by Δy and obeys the mass balance equation,

$$\Delta y = M_{\text{in}} - M_{\text{out}},$$

where M_{in} and M_{out} denote the amounts of sediment entering and leaving the cell, respectively.

3. TWO RIVAL NUMERICAL IMPLEMENTATIONS

Many mathematical models offer different numerical implementations which represent the physics of the problem from different perspectives. Alternative numerical implementations help test the model's robustness, since they only change the viewpoint from which one looks at the problem, but should not affect the results. For fluvial processes, the main rival numerical implementations are the Eulerian and the Lagrangian approach. The Eulerian approach describes the state of the system at fixed points in space and calculates subsequent states by synchronous updates of all mesh points. The Lagrangian method employs a moving frame of reference and describes the state of the system by particles that move with respect to each other [14].

The above cellular model lends itself to two different numerical implementations: the Eulerian approach and a method that compromises between the Eulerian and the Lagrangian approach. In the Eulerian approach, which operates on a fixed lattice, the amounts of water and sediment in each cell at time $k\Delta t$ are calculated from the corresponding amounts at the previous time $(k-1)\Delta t$ and the incoming and outflowing quantities during that time interval. If M^k is the quantity of a material in a cell at time $k\Delta t$ and $M_{\text{in}}^{(k,k+1)}$ and $M_{\text{out}}^{(k,k+1)}$ are the quantities entering and leaving the cell during the time interval $[k\Delta t, (k+1)\Delta t]$ respectively, then, the quantity M at time $(k+1)\Delta t$ is given by

$$M^{k+1} = M^k + M_{\text{in}}^{(k,k+1)} - M_{\text{out}}^{(k,k+1)}. \quad (2)$$

In the Eulerian approach, all grid cells are updated simultaneously during an iteration, so that one iteration corresponds to one time step $[k\Delta t, (k+1)\Delta t]$. The output after k iterations is the topography at time $k\Delta t$.

The second approach, which we call the marker-in-cell (MIC) method, also uses a fixed lattice. But instead of looking at the evolution of the entire lattice simultaneously, one moves with the quantities as they propagate along the lattice. One starts at the first lattice cell and updates the cell quantities as one propagates in the downstream direction. Thus, it only requires the initial fluxes at the upstream end of the study reach as model input, in contrast to the Eulerian approach, which requires initial flux values at all grid cells. We call the sequence of water and sediment distribution from the first to the last lattice column one *sweep*. In contrast to one iteration in the Eulerian method, one sweep is associated with several time steps. The material transfer between the first and second cells happens before the material transfer between consecutive cells. Thus, the MIC method provides direct answers to questions concerning the effects of events at one location on further downstream locations. Estimates of the bed profile at a given time $k\Delta t$ can also be calculated. Using the same notation as in equation (2), the quantity M in a cell changes twice during one sweep and satisfies the following system of equations,

$$\begin{aligned} M^{k+1} &= M^k + M_{\text{in}}^{(k,k+1)}, \\ M^{k+2} &= M^{k+1} - M_{\text{out}}^{(k+1,k+2)}, \end{aligned}$$

where M^{k+2} denotes the quantity M at the end of the sweep and the superscripts $(k, k+1)$ and $(k+1, k+2)$ correspond to the time intervals $[k\Delta t, (k+1)\Delta t]$ and $[(k+1)\Delta t, (k+2)\Delta t]$, respectively. The biggest difference between the two modeling approaches is the immediate update of cell elevations in the MIC method. This affects the local slopes and consequently the amounts of transferred sediment between adjacent cells. These discrepancies may cause essential differences in the model predictions. Such a lack of robustness would cast doubt on the whole modelling exercise.

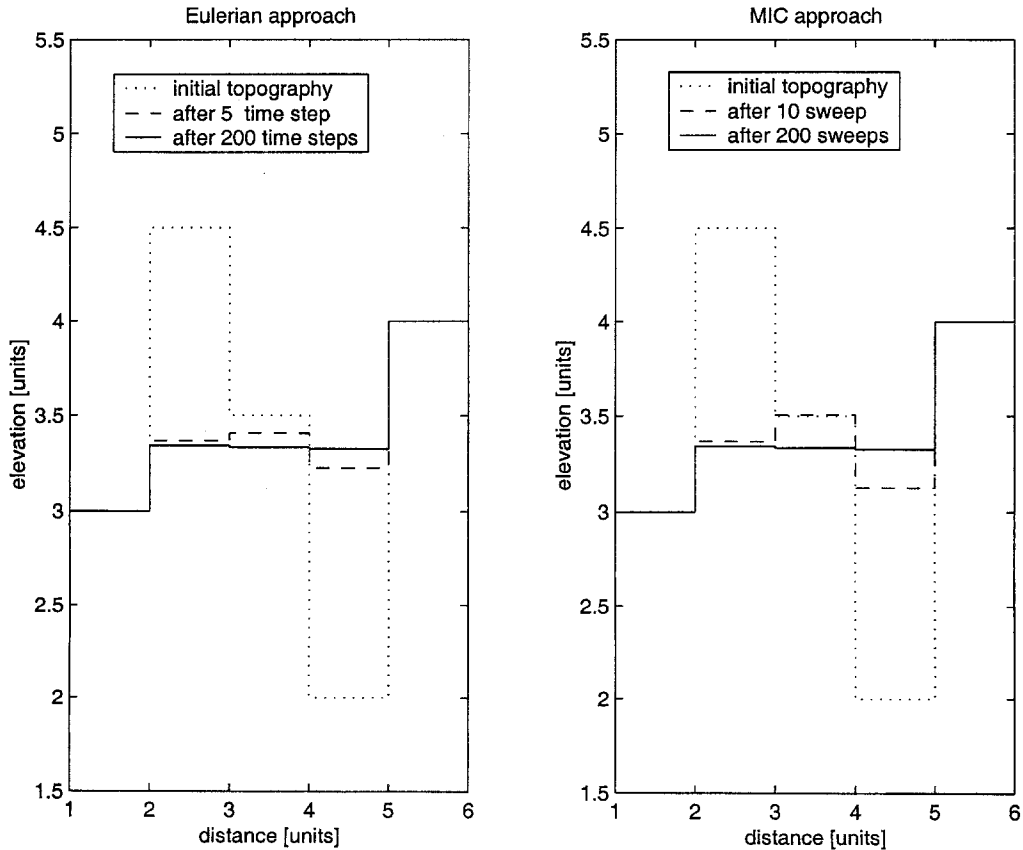


Figure 3. Time snapshots of the bed profile predicted by the Eulerian (left) and MIC method (right). The parameters used in this experiments were $K = 0.1$ and $m = 2$.

Figure 3 shows time snapshots of a river bed profile represented by a one-dimensional lattice of six cells, predicted by the Eulerian (left) and MIC approach (right). In this computational experiment, the Eulerian approach calculates a different profile at a given time than the MIC approach (dashed lines). However, both methods predict the same asymptotic behavior (solid lines). The lattice boundaries affect the long-term predictions of both approaches similarly, as is represented by the steps in the cell elevations after the first and before the last lattice cells. Various computational experiments for one- and two-dimensional lattices of different dimensions and for different parameter choices indicate that both approaches predict in general similar long-term behaviors. This study aims to support the observations from the numerical experiments by a more rigorous mathematical analysis.

4. DERIVATION OF PARTIAL DIFFERENTIAL EQUATIONS FROM BOTH NUMERICAL SCHEMES

4.1. Partial Differential Equation Associated With the Eulerian Approach

Let $y_i^n = y(i\Delta x, n\Delta t)$ denote the elevation of cell i at time $t_n = n\Delta t$, where Δx and Δt are the cell length and the time step in the numerical models. Taking cell dimension and time into account, the mass balance equation is

$$\frac{y_i^{n+1} - y_i^n}{\Delta t} \Delta x = K [H(-S_i^n)(-S_i^n)^m - H(-S_{i+1}^n)(-S_{i+1}^n)^m], \quad (4)$$

where

$$S_i^n = \frac{y_{i-1}^n - y_i^n}{\Delta x}$$

and $H(x)$ is the Heaviside step function, which is one, if $x \geq 0$ and zero, for $x < 0$. In the following, we will assume that the slopes S_i^n and S_{i+1}^n are always negative so that $H = 1$. If this is not the case, equation (4) does not yield a partial differential equation and modifications of the function H are required. We refer the discussion of the resulting complications to the concluding section of this paper. For $H = 1$, applying truncated Taylor series expansions in the limits $\Delta x \rightarrow 0$ and $\Delta t \rightarrow 0$ to equation (4) yields the differential equation,

$$\frac{\partial y}{\partial t} - Km \left(-\frac{\partial y}{\partial x} \right)^{m-1} \frac{\partial^2 y}{\partial x^2} = 0. \quad (5)$$

Equation (5) is a diffusion equation with diffusion coefficient $Km \left(-\frac{\partial y}{\partial x} \right)^{m-1}$. The Eulerian approach is known as the explicit difference scheme for solving the diffusion equation (see [15]).

4.2. Partial Differential Equation Associated With the Marker-In-Cell Method

The MIC-method involves three time levels during one sweep. Using the same notation as above, the mass-balance equation for cell i can be expressed as

$$\frac{y_i^{n+2} - y_i^n}{2\Delta t} \Delta x = K [H(-S_i^n)(-S_i^n)^m - H(-S_{i+1}^{n+1})(-S_{i+1}^{n+1})^m].$$

The terms in the above equation can be expanded into truncated Taylor series expansions at the mesh point $(i\Delta x, (n+1)\Delta t)$. If, as above, we assume that $H = 1$ and that $v = \Delta x/\Delta t$ is finite¹ yields, after taking the limits $\Delta t \rightarrow 0$ and $\Delta x \rightarrow 0$, the differential equation,

$$\frac{\partial y}{\partial t} = Km \left(-\frac{\partial y}{\partial x} \right)^{m-1} \frac{\partial^2 y}{\partial x^2} + \frac{Km}{v} \left(-\frac{\partial y}{\partial x} \right)^{m-1} \frac{\partial^2 y}{\partial x \partial t}. \quad (7)$$

¹In the following, we set $v = 1$, without loss of generality.

The first term on the right-hand side is the diffusion term that was obtained from the Euler method. The propagation of sediment, an explicit component in the cellular MIC method, results in the additional mixed derivative term in the MIC-partial differential equation. Understanding and interpreting the difference between the cellular Eulerian and MIC approach therefore reduces to the question: *How does the additional term on the right-hand side of equation (7) affect the solutions of the corresponding initial-value problem?*

The extra

$$\frac{Km}{v} \left(-\frac{\partial y}{\partial x} \right)^{m-1} \frac{\partial^2 y}{\partial x \partial t}$$

term transforms the parabolic diffusion equation (5) into a hyperbolic equation (7). Both parabolic and hyperbolic equations describe evolution processes, but hyperbolic equations are generally associated with the propagation of waves or signals, see [16]. The equations require different solution techniques and lead to solutions with different qualitative behaviors. In contrast to the Eulerian method, which is the well-known forward Euler method for solving the diffusion equation, the MIC-method cannot be identified as a familiar numerical solution scheme for approximating the solution of equation (7).

5. ANALYZING THE LINEAR PDES AND THEIR SOLUTIONS

For $m = 1$, the differential equations (5) and (7) are linear and analytic solutions can be obtained for appropriate initial and boundary conditions. The solution of the linear diffusion problem,

$$\begin{aligned} \frac{\partial y}{\partial t} &= K \frac{\partial^2 y}{\partial x^2}, \\ y(x, 0) &= y_0(x), \end{aligned} \quad (8)$$

with an integrable real function y_0 is

$$y(x, t) = \frac{1}{\sqrt{4\pi Kt}} \int_{-\infty}^{\infty} y_0(u) e^{-(x-u)^2/4Kt} du. \quad (9)$$

Hyperbolic linear second-order partial differential equations generally require two initial conditions for a unique solution. However, a unique solution can be obtained for the following initial-boundary value problem that uses one initial condition and a weak boundary condition at infinity

$$\begin{aligned} \frac{\partial y}{\partial t} &= K \left(\frac{\partial^2 y}{\partial x^2} + \frac{\partial^2 y}{\partial x \partial t} \right), & \text{for } x \in \mathbb{R}, \quad t > 0, \\ y(x, 0) &= y_0(x), & \text{for } x \in \mathbb{R}, \\ \lim_{|x| \rightarrow \infty} |y(x, t)| &< \infty, & \text{for } t \geq 0, \end{aligned} \quad (10)$$

for a continuous, differentiable, bounded real-valued function y_0 (see [17]). The solution of the above problem was derived in [17] and has the form,

$$y(x, t) = \int_{-\infty}^t g(x-u) e^{(u-2t)/K} I_0 \left(\frac{2}{K} \sqrt{t(t-u)} \right) du, \quad (11)$$

where

$$g(x) = \frac{1}{K} y_0(x) - y'_0(x)$$

and I_0 is the modified Bessel function of the first kind of order zero.

At first glance, the analytical solutions (9) and (11) of the linear diffusion and MIC equations do not appear similar. For example, for fixed times $t > 0$, the solution of the linear diffusion equation is an even function in x provided the initial function $y_0(x)$ is even. In contrast, the solution of

the MIC equation involves the integration over the interval $(-\infty, t]$ indicating a nonsymmetrical temporal evolution of an even initial function. Despite this, in [17] it is shown that the exact solutions of systems (8) and (10) rapidly converge to each other as time increases. Further, for finite times and bounded initial functions with bounded first derivatives, the discrepancy between both solutions is also bounded.

Figure 4 shows time snapshots of the analytic solutions (left) of the initial value problems (8) and (10) and of the corresponding difference function $e(x, t)$ (right) for different initial functions y_0 . As flow propagates over the undulations, they spread out and decrease in altitude. The analytical solutions greatly resemble one another and the magnitude of the difference function decreases as time increases. The mixed derivative term in the MIC equation can be identified as a process that inhibits the symmetric evolution of the initial function, which is controlled by the diffusion process. But compared to the diffusion process, this inhibiting process is very weak.²

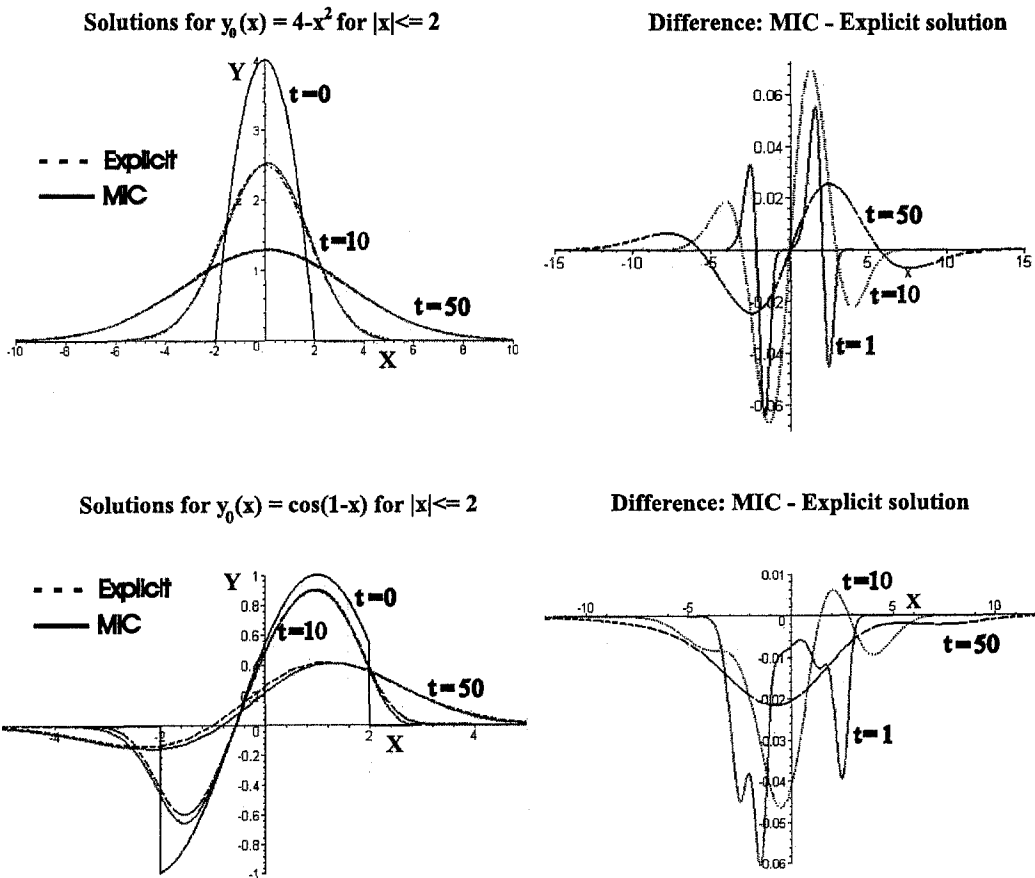


Figure 4. Time snapshots of the solutions for the MIC and Euler equation for different initial functions (left) and of their differences (right).

5.1. Assessment of the Linear Numerical Eulerian and MIC Schemes

The quality of finite difference schemes for approximating solutions of partial differential equations is determined by the following four criteria: accuracy of the numerical solutions, consistency and convergence of the schemes as well as stability, see [15]. The accuracy of solutions is determined by the local truncation errors at the mesh-points $(i\Delta x, n\Delta t)$. A scheme is consistent if the solution of the difference equation converges to the solution of the differential equation as the mesh lengths tend to zero and convergent, if the discretization error $e_i^n = Z_i^n - z_i^n$, between the

²The study of the MIC equation revealed that the hyperbolic MIC equation shares some properties with parabolic equations. This observation is interesting in its own right and is investigated by two of the authors in [17].

exact solutions Z_i^n and z_i^n of the differential and difference equations at the $(i, n)^{\text{th}}$ mesh-point converges to zero, for all i and n . Stability refers to a limited amplification of all components of the initial conditions. For linear finite difference schemes, methods to assess the validity of all four criteria are well established. Assessment of the explicit (Eulerian) method as solution scheme of the linear diffusion initial-value problem according to the above criteria can be found in standard textbooks (e.g., [15]) and is summarized in the top row of Table 1. Substitution of the exact solution of the linear MIC equation into the finite difference equation (6) yields the local truncation errors and the result for consistency for the MIC scheme, as presented in the second row in Table 1. Lax-Richtmyer's definition of stability [15] yields that the linear MIC scheme is unstable and, hence, not convergent. Nevertheless, applying von Neumann's Fourier-series method, it can be shown that the amplification rate of the round-off errors is small (i.e., for

$$\frac{K\Delta t}{(\Delta x)^2} < \frac{1}{2},$$

the stability condition for the linear explicit scheme, round-off errors grow at a rate less than $\sqrt{5}$), suggesting that the MIC model is valid for a finite time span (see Figure 5). According to these criteria, the Eulerian method is better than the MIC method on three counts: it has a lower truncation error, it is conditionally stable, and it is convergent. The MIC method is still a valid solution method if predictions are made over sufficiently small time spans.

Table 1. Evaluation of the linear numerical difference schemes according to four criteria.

Criterion/Scheme	Local Truncation Error	Consistent	Convergent	Stable
Euler	$O(\Delta t) + O(\Delta x^2)$	yes	yes	if $\frac{K\Delta t}{(\Delta x)^2} < 0.5$
MIC	$O(\Delta t) + O(\Delta t^2)$	yes	no	no, but bounded $O(\Delta x^2)$ growth of errors

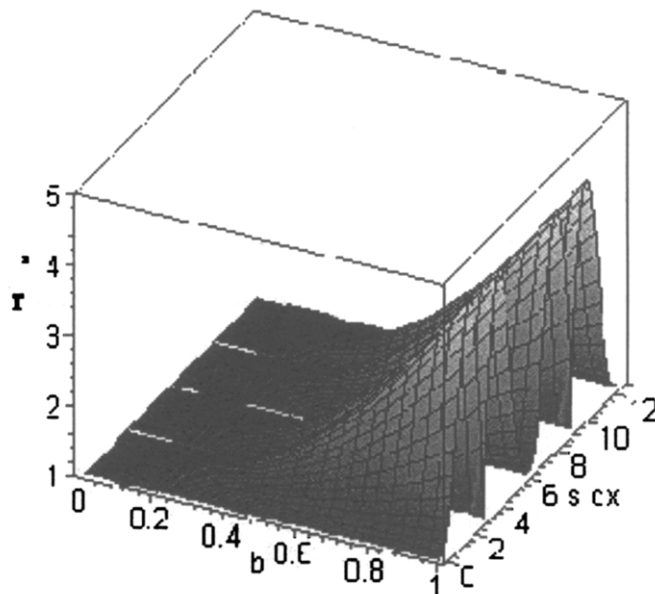


Figure 5. Amplification factor r^2 of the round-off errors in the MIC model as function of $b = K\Delta t/(\Delta x)^2$ and $s\Delta x$, where $s = \pi/N\Delta x$.

6. ANALYZING THE NONLINEAR PDES AND THEIR NUMERICAL SOLUTIONS

Most natural phenomena represent nonlinear relationships between interacting components. In our study, the components are water and sediment flux. An exaggerated nonlinear response

of sediment to water flux is crucial for topographic changes in many rivers (see [7]). For $m > 1$, the PDEs (5) and (7) cannot be solved analytically and most methods devised to assess the numerical linear solution schemes are inapplicable. The quality of the nonlinear Eulerian and MIC schemes will be assessed by comparing them with other numerical solution schemes for the corresponding PDEs. Although the analysis of the nonlinear numerical schemes is less rigorous than the analysis of the linear counterparts, insight into model behaviors is still obtained.

6.1. Numerical Solutions of the Nonlinear Diffusion Initial-Value Problem

An alternative numerical solution of the nonlinear initial-value diffusion problem

$$\frac{\partial y}{\partial t} = Km \left(-\frac{\partial y}{\partial x} \right)^{m-1} \frac{\partial^2 y}{\partial x^2}, \quad (12)$$

$$y(x, 0) = y_0(x), \quad (13)$$

with $m \neq 1$ can be obtained using similarity transformations (see [18]). The above system has stretching symmetry provided

$$y_0(\lambda x) = g(\lambda) y_0(x), \quad (14)$$

for every real constant λ and a real function g . In particular, functions of the form,

$$y_0(x) = Ax^a,$$

satisfy the above condition. The restriction to a finite domain or additional boundary conditions, however, would break the stretching symmetry. The stretching symmetry of the initial value problem (12),(13) yields similarity transformations of the system's variables, which transform the above initial value problem into an ordinary differential equation boundary-value problem. As the transformation depends on the initial values, we restrict the assessment to two specific examples where the initial function $y_0(x) = y(x, 0)$ satisfies condition (14). For the purpose of this study, we consider the following initial conditions,

$$y(x, 0) = \begin{cases} k_1, x, & \text{for } x < 0, \\ k_2, x, & \text{for } x \geq 0, \end{cases} \quad (15)$$

and

$$y(x, 0) = \begin{cases} A\sqrt{-x}, & \text{for } x < 0, \\ -A\sqrt{x}, & \text{for } x \geq 0, \end{cases} \quad (16)$$

where k_1 and k_2 are negative constants and A is a positive constant. Problems (12),(15) can be solved with the transformations,

$$\begin{aligned} r &= t^{-1/2}x, \\ Y(r) &= t^{-1/2}y(x, t), \end{aligned}$$

and

$$\begin{aligned} r &= t^{-1/2}x, \\ U(r) &= u(x, t), \end{aligned}$$

where $u(x, t) = \frac{\partial y}{\partial x}(x, t)$. These yield, after substitution into equations (12),(15), the system of first-order ordinary differential equations

$$\begin{aligned} Y' &= U, \\ U' &= \frac{Y - rU}{2Km(-U)^{m-1}}, \end{aligned} \quad (17)$$

with boundary conditions,

$$\begin{aligned} Y(-\infty) &= \infty, & U(-\infty) &= -k_1, \\ Y(\infty) &= -\infty, & U(\infty) &= k_2. \end{aligned} \quad (18)$$

Instead of the partial differential equation (12) with initial conditions (15), we now have to solve the first-order system of ordinary differential equations (17) with boundary conditions (18). The problematic infinite boundary points can be overcome using the shooting method (see [19]), in which constants $Y_0 = Y(0)$ and $U_0 = U(0)$ are sought that yield the correct behavior of U and Y at $\pm\infty$. The same techniques applied to the initial value problem (12),(16) give rise to the similarity transformations,

$$\begin{aligned} r &= t^{-2/(m+3)}x, \\ Y(r) &= t^{-1/(m+3)}y(x, t), \\ U(r) &= |r|^{-1/2}Y(r), \end{aligned}$$

and yield after substitution the second-order ordinary differential equation,

$$\frac{2}{m+3} |r|^{2/3} U'(r) + KM \left(\left(-\sqrt{|r|} U(r) \right)' \right)^{m-1} \left(\sqrt{|r|} U(r) \right)'' = 0, \quad (19)$$

with constant boundary conditions,

$$\begin{aligned} \lim_{r \rightarrow -\infty} U(r) &= A, \\ \lim_{r \rightarrow \infty} U(r) &= -A. \end{aligned} \quad (20)$$

By transforming the original problems (12) with initial conditions (15),(16), respectively to the boundary value problems (17),(18) and (19),(20), more sophisticated numerical solution schemes can be applied to estimate the solution of the original problems. Numerical similarity solutions to solve the boundary value problems (17),(18) and (19),(20) were obtained by the solution method *dverk78*—a seventh to eighth order Runge-Kutta method (see [20]) in the software package MAPLE 6. Amongst the variety of numerical solvers incorporated into MAPLE 6, *dverk78* presented the best compromise between calculation time and error tolerance. The presented numerical results correspond to an error tolerance of 10^{-8} .

The Eulerian method operates on a finite spatial domain. To allow the comparison with the numerical similarity solutions, the influence of the domain boundaries for the explicit (Eulerian) method was minimized by calculating the solutions for a large spatial domain (i.e., $x \in [-500, 500]$) without fixing the elevations at the boundaries. Then, the comparison with the approximated similarity solutions was performed for a relatively small range of x values (i.e., $x \in [-10, 10]$) far away from the boundaries. In Section 6.3, the numerical similarity solutions are compared with the solutions of the much simpler Eulerian method.

6.2. Numerical Solutions of the Nonlinear MIC Initial-Value Problem

The MIC initial value problem,

$$\frac{\partial y}{\partial t} = Km \left(-\frac{\partial y}{\partial x} \right)^{m-1} \left(\frac{\partial^2 y}{\partial x^2} + \frac{\partial^2 y}{\partial x \partial t} \right), \quad (21)$$

$$y(x, 0) = y_0(x), \quad (22)$$

also has stretching symmetry for particular initial functions. However, the resulting differential equation contains singularities, which disable the application of the shooting method to estimate

starting points for the numerical schemes. For this reason, we aimed to construct a finite difference scheme that satisfies the same initial and boundary conditions as the MIC method. These criteria hold for an implicit scheme that uses forward difference approximations for the derivatives, $\frac{\partial y}{\partial t}$ and $\frac{\partial y}{\partial x}$, respectively, and a central difference approximation for $\frac{\partial^2 y}{\partial x^2}$. The mixed derivative, $\frac{\partial^2 y}{\partial x \partial t}$, at the $(i, n)^{\text{th}}$ mesh-point is approximated by

$$\left. \frac{\partial^2 y}{\partial x \partial t} \right|_{(i, n)} \sim \frac{1}{\Delta x \Delta t} (y_i^{n+1} - y_i^n - y_{i-1}^{n+1} + y_{i-1}^n).$$

In contrast to the above similarity solutions, the implicit scheme operates like the MIC and Eulerian scheme on finite domains. For specified values at the boundaries $x = 0$, $x = L$, and $t = 0$, the implicit scheme calculates the values of the interior mesh-points via

$$L(y_i^n, y_{i+1}^n) y_i^{n+1} = R(y_{i-1}^n, y_i^n, y_{i+1}^n, y_{i-1}^{n+1}),$$

where L and R are the nonlinear functions

$$\begin{aligned} L &= 1 - \frac{Km}{\Delta x} \left(\frac{y_i^n - y_{i+1}^n}{\Delta x} \right)^{m-1} \\ R &= y_i^n + \frac{Km\Delta t}{(\Delta x)^2} \left(\frac{y_i^n - y_{i+1}^n}{\Delta x} \right)^{m-1} (y_{i-1}^n - 2y_i^n + y_{i+1}^n) \\ &\quad + \frac{Km}{\Delta x} \left(\frac{y_i^n - y_{i+1}^n}{\Delta x} \right)^{m-1} (y_{i-1}^n - y_i^n - y_{i-1}^{n+1}). \end{aligned}$$

6.3. Numerical Results

The same criteria applied to the linear schemes are used to assess the nonlinear Eulerian, Runge-Kutta, MIC and implicit methods. The domain for comparing the Eulerian and similarity solutions was defined in Section 6.1. The three finite difference schemes (Eulerian, MIC and implicit) operate on a finite domain. In order to compare the three methods, the initial conditions (15),(16) were modified to the following set of initial-boundary conditions

$$y(x, 0) = \begin{cases} k_1 x, & \text{for } -10 \leq x < 0, \\ k_2 x, & \text{for } 0 \leq x \leq 10, \end{cases} \quad (23)$$

$$\begin{aligned} y(-L, t) &= k_1 L, \\ y(L, t) &= -k_2 L, \end{aligned} \quad (24)$$

and

$$y(x, 0) = \begin{cases} A\sqrt{-x}, & \text{for } -10 \leq x < 0, \\ -A\sqrt{x}, & \text{for } 0 \leq x \leq 10, \end{cases} \quad (25)$$

$$\begin{aligned} y(-L, t) &= A\sqrt{L}, \\ y(L, t) &= -A\sqrt{L}, \end{aligned} \quad (26)$$

with the same constants k_1 , k_2 , and A as in equations (15),(16). Instead of fixed boundary values, we could have also used zero or constant flux conditions at the boundaries of the spatial domain.

COMPARISON OF THE NUMERICAL RESULTS. Time snapshots of the approximated solutions to the nonlinear diffusion and MIC problems for the above initial conditions are presented in Figures 6 and 7, respectively. All applied numerical schemes predict the evolution of the initial topographies towards a straight line. However, while the time snapshots corresponding to the numerical similarity solutions and the solutions of the explicit scheme are indistinguishable, a

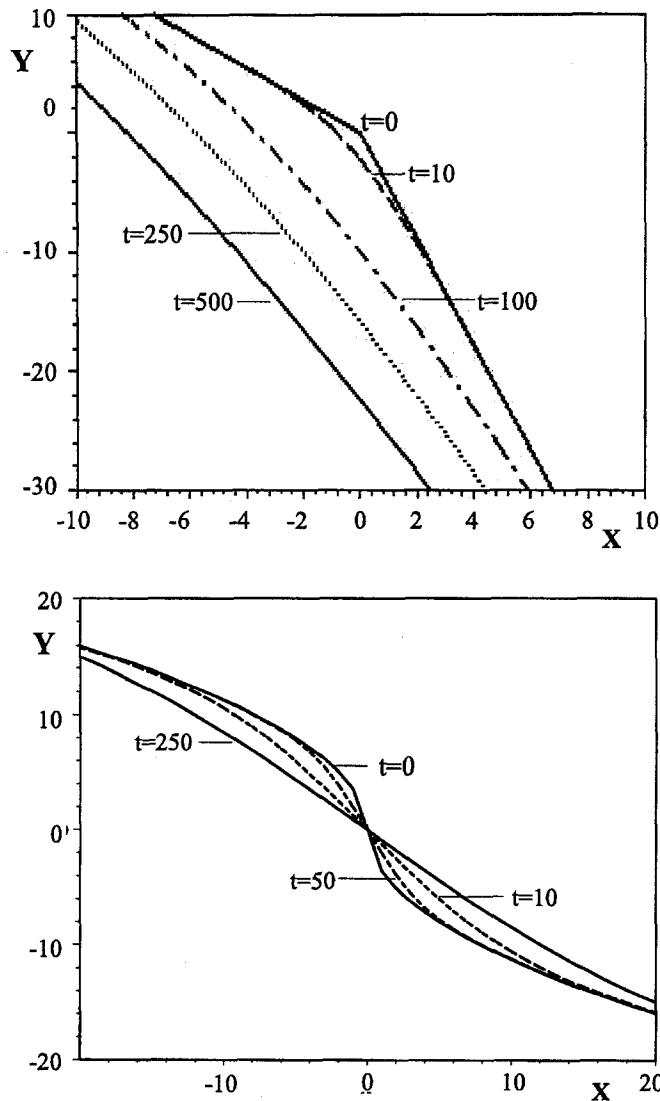


Figure 6. Time snapshots of the approximated solutions of the nonlinear diffusion equation with initial function (15) (top) and (16) (bottom) for step sizes $\Delta x = \Delta t = 0.5$. The constants are $m = 5/3$, $k_1 = -1.4$, $k_2 = -4.5$ and $K = 0.01$ (top) and $A = 3.56$ and $K = 0.1$ (bottom). The similarity solutions and the solutions of the Eulerian method are visually indistinguishable.

significant discrepancy between the solutions of the MIC scheme and the implicit scheme can be detected (solid versus dotted lines in Figure 7).

ACCURACY OF THE NUMERICAL SCHEMES. The local truncation errors of the finite difference schemes are

$$T_i^n = \begin{cases} O(\Delta t) + O(\Delta x^2) & \text{(Euler)} \\ O(\Delta t) + O(\Delta t^2) + O(\Delta x^2) & \text{(MIC)} \\ O(\Delta t) + O(\Delta x) & \text{(Implicit)} \end{cases}$$

and imply that the explicit method is more accurate than the MIC method and that the latter is more accurate than the implicit scheme. To compare these accuracies with the accuracy of the similarity solutions, a discrepancy function $D(t)$ between the solutions \hat{y} and \tilde{y} of two numerical schemes was defined by

$$D(t) = \max_{i \in I} \{|\hat{y}(x_i, t) - \tilde{y}(x_i, t)|\},$$

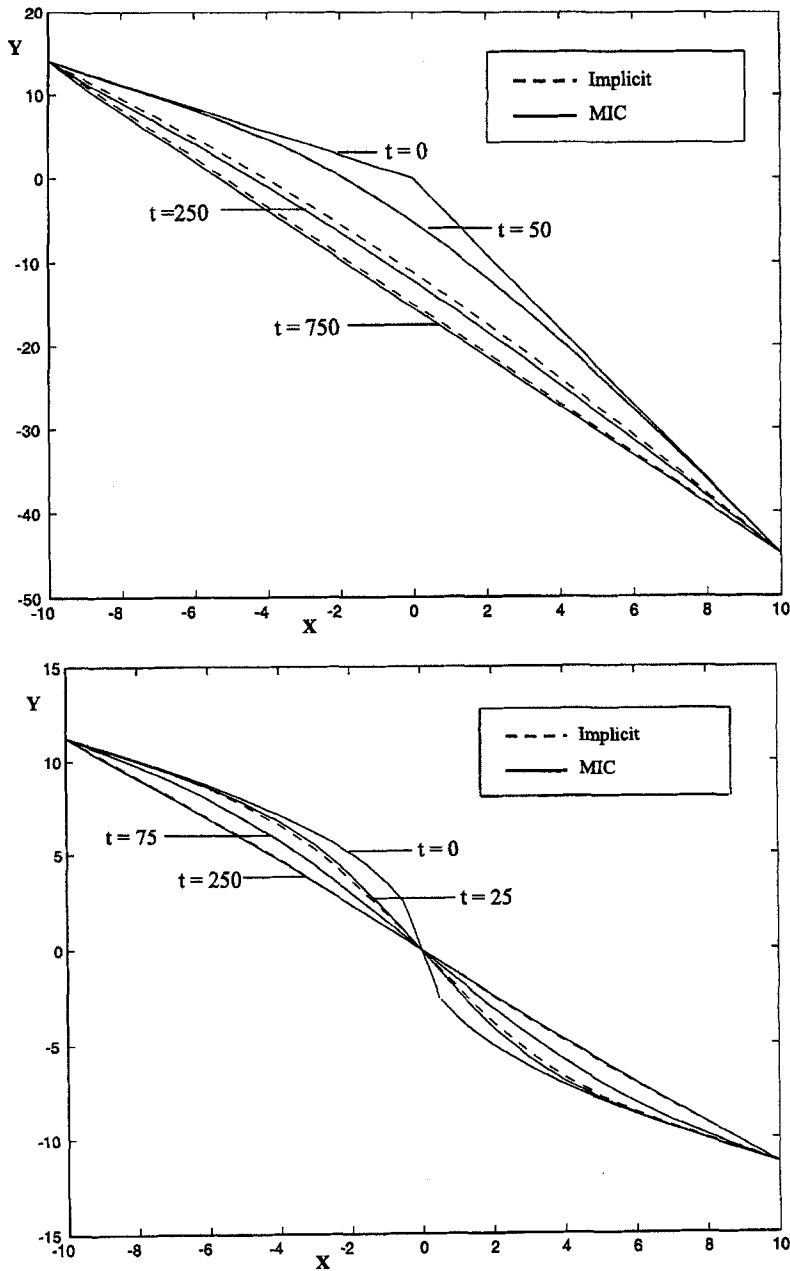


Figure 7. Time snapshots of the approximated solutions of the nonlinear diffusion equation with initial function (23),(24) (top) and (25),(26) (bottom) for step sizes $\Delta x = \Delta t = 0.5$. The constants are $m = 5/3$, $k_1 = -1.4$, $k_2 = -4.5$ and $K = 0.01$ (top) and $A = 3.56$ and $K = 0.1$ (bottom). The similarity solutions and the solutions of the Eulerian method are visually indistinguishable.

where I denotes the set of x -values for which both solutions were obtained. Figure 8 shows that for $\Delta x = \Delta t = 0.5$, the maximal discrepancy between the solutions of the Eulerian and the similarity method at fixed t -values has order 10^{-2} for values of t between 0 and 500 and x in $[-10, 10]$ (top left graph). The discrepancy is surprisingly small considering the variety of errors introduced by the shooting method and the numerical solver in MAPLE in the numerical similarity solutions as well as the local truncation error of the Eulerian solution. The maximal discrepancies between the finite difference solutions, in particular between the solutions of the implicit scheme and the cellular schemes, are significantly higher (see Figure 8).

STABILITY AND CONVERGENCE. For the corresponding linear problems, the Eulerian method was conditionally stable and the MIC method was unstable with a relatively small amplification

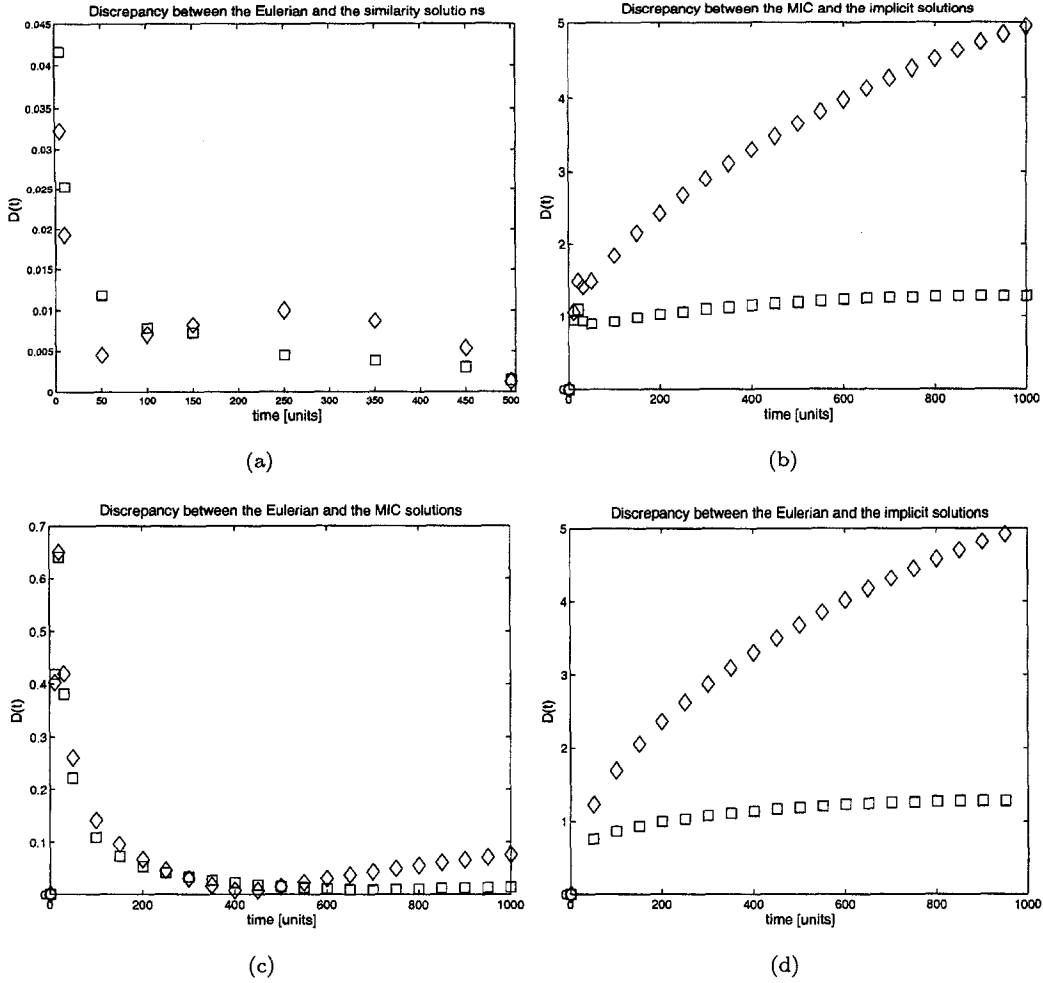


Figure 8. Maximal discrepancies between the solutions of different schemes. Diamonds refer to initial conditions (15) for the top left graph and (23) for the remaining graphs, respectively. Squares refer to the initial conditions (16) and (25) respectively. All runs used the same step sizes $\Delta x = \Delta t = 0.5$ and constants $K = 0.01$ and $m = 5/3$.

factor. Since rigorous general methods for assessing the stability of nonlinear solution schemes do not exist (see [21]), assessment of stability of the numerical methods is tackled by empirical means. These rely on the observation that the symptom of instability of the finite difference schemes are oscillations with temporally increasing amplitudes. Stability depends on the parameter K , and the step sizes Δx and Δt . Using fixed step sizes $\Delta x = \Delta t = 0.5$ for the finite difference schemes and varying exponent m , the largest value of the scaling constant K was computed, for which oscillations occurred within 10,000 time steps. Under the assumption that the absence of oscillations indicates stability of the finite difference schemes, the following observations were made (see Figure 9).

- (1) Stability depends partly on the initial conditions.
- (2) For all difference schemes, stability decreases with increasing exponent m . Combined with the results for the linear method, this observation implies instability for the nonlinear MIC scheme and at most a conditional stability for the nonlinear Eulerian scheme with stricter conditions than for the linear Eulerian scheme. The separation line between the stable and unstable region approximately satisfies the inverse logarithmic relationship

$$\log_{10}(K) \propto \frac{1}{m}.$$

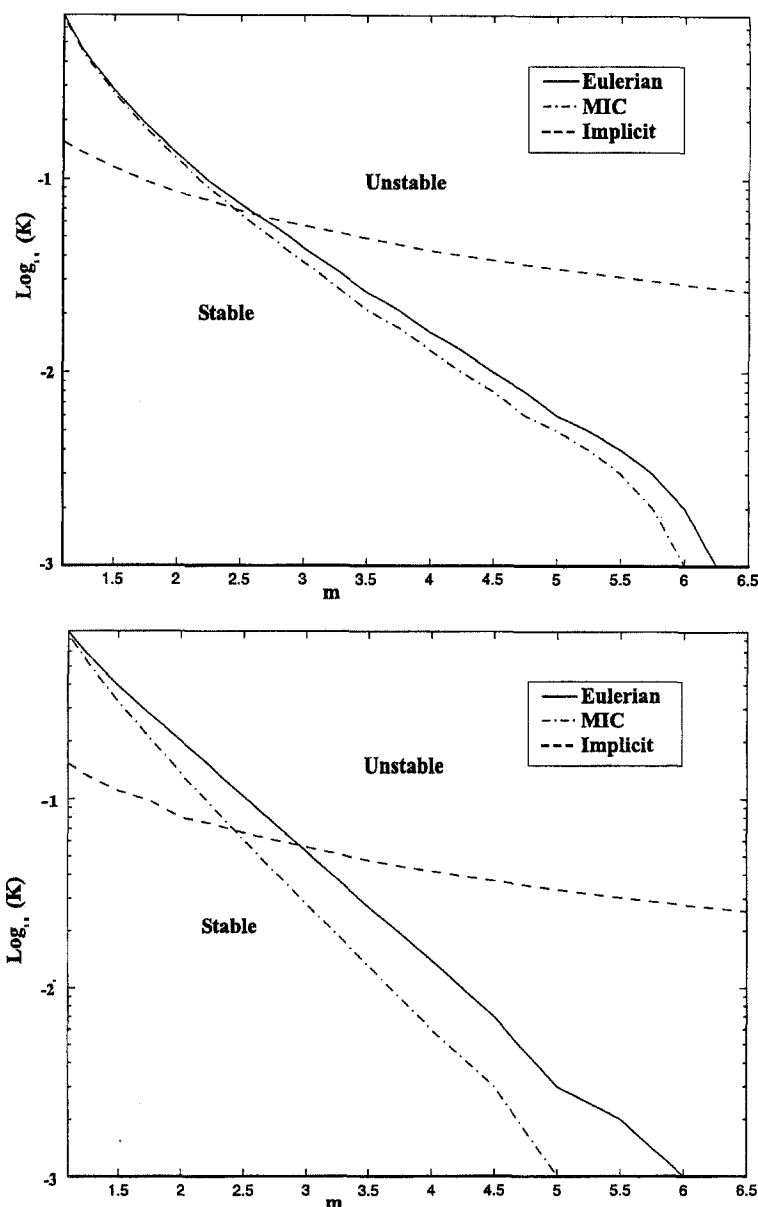


Figure 9. Relationship between the constants m and K for stability of the nonlinear Eulerian, MIC and implicit schemes. The top figure refers to initial conditions (23), (24), the bottom figure refers to initial conditions (25), (26).

- (3) The Eulerian method is always more stable than the MIC method. For relatively small m (i.e., $m \leq 2.5$ in Section 6.3), both, the MIC and Eulerian method are more stable than the implicit method. For larger m , the contrary is true.

The instability of the numerical Runge-Kutta scheme used to calculate the approximate similarity solutions, does not manifest itself in oscillating solutions. Although for some values of m and K in the unstable region of the Eulerian method, starting points $(Y(0), U(0))$ yielding the appropriate boundary conditions could not be obtained, numerical experiments with different K -values indicate that the Runge-Kutta method devised for the similarity solutions is more stable than the other presented schemes.

The convergence of the Runge-Kutta scheme (see [22]) and the strong agreement between the solutions of the nonlinear Eulerian and Runge-Kutta schemes in the common stability region suggests that the nonlinear Eulerian scheme is also convergent when stable. Since the linear MIC scheme is not convergent, we deduce that the nonlinear MIC method is also not convergent.

7. DISCUSSION AND CONCLUSIONS

The main goal of this study was to demonstrate how partial differential equations can be used to assess numerical models arising from a cellular automata approach. The study focused on two rival numerical models for morphological processes in river beds and addressed the following questions. How do the models differ in their predictions and what are the advantages of each approach? Can these simple numerical models compete with more sophisticated numerical schemes that model the same processes?

The relationship between the numerical cellular automata based models and partial differential equations was established by viewing the models as numerical solution schemes of partial differential equations with initial and boundary values derived from the governing equations of the cellular models. This viewpoint conversion revealed that both models, when reduced to one dimension, have a strong diffusive component. The difference between the models consists of an additional expression in the MIC partial differential equation, represented by a second-order mixed derivative term. Understanding the difference between the numerical models boiled down to understanding the impact of this additional term in the MIC equation.

The foundations of this study were laid by analyzing the linear equations and solution procedures ($m = 1$) using a variety of established techniques. We could prove that the exact solutions of both problems are very similar and eventually converge. This implies that the additional, mixed derivative term in the MIC equation has negligible influence on the model predictions and confirms the observations from numerical experiments. It implies that the linear cellular automata based model is robust to different numerical implementations. Computational experiments suggest that these results are also valid for the nonlinear models in one and two dimensions. Further, we could show that the Eulerian method to solve the linear diffusion initial-value problem is more accurate and more stable than the MIC method for solving the MIC initial-boundary value problem. The combined results of the rigorous linear and the more empirical nonlinear analysis suggest that the Eulerian approach is somewhat better than the MIC approach for modeling the temporal evolution of a longitudinal river profile. However, although the MIC method is less accurate and unstable, it produces good results for a limited time with sufficiently small time steps. The MIC model is, therefore, a valid approach if conditions are only known at an upstream region of the river or if phenomena, such as the impact of upstream events on downstream regions, are investigated.

Comparison with other numerical schemes to solve the corresponding nonlinear partial differential equations shed light onto the advantages of both cellular models. As an alternative to the Eulerian model to solve the nonlinear diffusion initial-value problem, the similarity method combined with sophisticated numerical ODE solvers was applied. Although these procedures appear more stable and may generate solutions of greater accuracy, their application is restricted to certain initial and boundary conditions. The Eulerian model, on the contrary, generates solutions which differ little from those of the more sophisticated scheme, but can be applied to a wide range of initial and boundary conditions. To solve the nonlinear MIC equation, we developed an implicit scheme that satisfies the same initial and boundary conditions as the MIC scheme. The implicit scheme required similarly little computational effort as the explicit Eulerian and MIC schemes, but was trumped by the latter in accuracy and, for $m < 2.5$, also in stability. In summary, for the one-dimensional initial and initial-boundary value problems, for which alternative numerical models could be applied, the cellular models performed well.

The fact that the cellular models are valid schemes to model simple processes, encourages the application of these models to more complicated, higher-dimensional problems. However, since the original cellular models of this study were two dimensional and applied to all initial topographies, it would be desirable to extend the present analysis to two dimensions and to lift the restriction to negative slopes. The latter could be achieved by replacing the Heaviside step

functions in equations (4) and (6) by the differentiable function,

$$H(x) = \frac{1}{2} (1 + \tanh(ax)),$$

where the constant a determines the slope of the curve near $x = 0$. The resulting, more complicated, differential equations apply for all local slopes and approximate the derived diffusion and MIC equation when a is large.

Deriving partial differential equations from the two-dimensional numerical models is also possible, but involves the consideration of water and sediment transport and the inclusion of six instead of two neighbors. In contrast to the one-dimensional cellular automata based model, discharge is no longer constant in two dimensions, but depends on the local slopes, so that the models relate to systems of differential equations instead of one differential equation. The additional inclusion of more cell neighbors yields more terms in the mass balance equations. The differential equations resulting from these extensions, therefore, are significantly more complicated than the one-dimensional initial value problems considered in this study and are not likely to serve as a means to gain insights into the cellular models. They rather confirm the advantage of the cellular approach as a tool to model processes that are difficult to model by other means.

REFERENCES

1. S. Wolfram, Universality and complexity in cellular automata, *Physica D* **10**, 1–35, (1984).
2. A.B. Murray, Contrasting the goal, strategies, and predictions associated with simplified numerical models and detailed simulations, In *Prediction in Geomorphology, Geographical Monograph 135, American Geophysical Union*, (Edited by Dick Iverson and Peter Wilcock), pp. 151–165, (2003).
3. B. McArdell and R. Faeh, A computational investigations of river braiding, In *Gravel-bed Rivers 5*, Hydrological Society, Inc., Wellington, New Zealand, (2000).
4. G.B. Ermentrout and L. Edelstein-Keshet, Cellular automata approaches to biological modeling, *J. Theor. Biol.* **160**, 97–133, (1993).
5. A.B. Murray and C. Paola, A cellular model of braided rivers, *Nature* **371**, 54–57, (1984).
6. T.J. Coulthard, M.J. Kirkby and G.M. Macklin, *Fluvial Processes and Environmental Change*, John Wiley and Sons Ltd., (1999).
7. C. Paola, *Gravel-bed Rivers 5*, Hydrological Society, Inc., Wellington, New Zealand, (2000).
8. A.B. Murray and C. Paola, Properties of a cellular braided stream model, *Earth Surface Processes and Landforms* **22**, 1001–1025, (1997).
9. A.B. Murray and C. Paola, A new quantitative test of geomorphic models, applied to a model of braided streams, *Water Resources Research* **32** (8), 2579–2587, (1996).
10. V. Sapozhnikov, A.B. Murray, C. Paola and E. Foufoula-Georgiou, Validation of braided-stream models: Spatial state-space plots, self-affine scaling and island shape comparison, *Water Resources Research* **34** (9), 2353–2364, (1998).
11. A. Doeschl, Assessing Braided River Dynamics With a Cellular Model, Ph.D. Dissertation, University of Western Ontario, Canada, (2000).
12. F. Engelund and E. Hansen, *A Monograph of Sediment Transport in Alluvial Streams*, Teknisk Forlag, Copenhagen, (1967).
13. P. Ashmore, Process and form in gravel braided streams: Laboratory modelling and field observations, Ph.D. Dissertation, University of Alberta, Canada, (1985).
14. D.M. Tetzlaff and J.W. Harbaugh, *Simulating Clastic Sedimentation*, Van Norstrand Reinhold, New York, (1989).
15. G.D. Smith, Numerical solution of partial differential equations: Finite difference methods, In *Oxford Applied Mathematics and Computing Science Series*, Third Edition, Oxford University Press, (1985).
16. J.D. Logan, *An Introduction to Nonlinear Partial Differential Equations*, John Wiley and Sons, Inc., (1988).
17. M. Davison and A. Doeschl, A hyperbolic PDE with parabolic behaviour, *SIAM Review* **46** (1), 115–127, (2004).
18. L. Dresner, *Similarity Solutions of Nonlinear Partial Differential Equations*, Springer-Verlag, New York, (1983).
19. L.W. Johnson and R.D. Riess, *Numerical Analysis*, Chapter 7.8.2, Addison-Wesley Publishing Company, (1982).
20. W.H. Enright, The relative efficiency of alternative defect control schemes for high order continuous Runge-Kutta formulas, Technical Report 252/91, Department of Computer Science, University of Toronto, Canada, (1991).
21. W.F. Ames, *Numerical Methods for Partial Differential Equations*, Academic Press, Inc., (1992).
22. J.H.E. Cartwright and P. Oreste, The dynamics of Runge-Kutta methods, *Int. J. Bifurcation and Chaos* **2**, 427–449, (1992).